Biochemical and Biophysical Research Communications 422 (2012) 8–14

Contents lists available at SciVerse ScienceDirect

Biochemical and Biophysical Research Communications

journal homepage: www.elsevier.com/locate/ybbrc

Proteomic analysis reveals a protective role for DJ-1 during 6-hydroxydopamine-induced cell death

Su-Jeong Kim, Yun-Jong Park, Young J. Oh *

Department of Systems Biology, Yonsei University College of Life Science and Biotechnology, Seoul 120-749, Republic of Korea

ARTICLE INFO

Article history:
Received 11 April 2012
Available online 21 April 2012

Keywords:
DJ-1/PARK7
Proteomics
6-Hydroxydopamine
Parkinson's disease

ABSTRACT

Loss-of-function mutations in the DJ-1/PARK7 gene are responsible for early-onset autosomal-recessive Parkinson's disease. DJ-1 is implicated in the protection of neurons from oxidative stress by scavenging hydrogen peroxide and regulating the transcriptional activity of multiple pathways. Here, we attempted to identify the protein profiles modulated by DJ-1 in MN9D dopaminergic neurons following 6-hydroxydopamine (6-OHDA) treatment. We found that reactive oxygen species (ROS) levels increased in DJ-1-deficient cells that were either untreated or subjected to 6-OHDA treatment. The incidence of apoptosis after 6-OHDA treatment was increased in DJ-1 knockdown cells. Using these cells, we then performed two-dimensional gel electrophoresis in conjunction with mass spectrometry to assess changes in protein profiles before and after 6-OHDA treatment. Several protein spots were positively or negatively altered in DJ-1-deficient cells with or without 6-OHDA. Among the altered proteins, immunoblot analysis confirmed an increase in galectin-7 and a decrease in peroxiredoxin-6 in DJ-1 knockdown cells. Moreover, transcriptional levels of putative p53 target proteins, including selenophosphate synthetase 1 and glycogen phosphorylase, were increased in the DJ-1 knockdown cells. Taken together, our data suggest that increases in pro-apoptotic proteins and decreases in anti-apoptotic proteins render DJ-1 knockdown cells more susceptible to oxidative stress.

1. Introduction

Parkinson's disease (PD) is caused by the loss of dopaminergic neurons in the substantia nigra, and the resulting depletion of dopamine in the striatum evokes motor symptoms [1]. Although most cases of PD are idiopathic, mutations in specific genes are involved in familial cases [2]. For example, DJ-1, also known as PARK 7, was discovered as the third locus for an early-onset autosomal-recessively inherited form of PD [3]. DJ-1 deletion or missense mutations leading to a loss of function have been identified in Italian and other European families [4]. DJ-1 is a ubiquitous redox-responsive chaperone protein with multiple functions [5]. At the subcellular level, DJ-1 has been shown to translocate into the mitochondria in response to MPP^+, and loss of DJ-1 leads to a loss of mitochondrial membrane potential and the fragmentation of mitochondria [6], suggesting that DJ-1 is crucial for maintaining mitochondrial integrity [7,8]. DJ-1 has also been suggested to play an active role as a neuroprotective transcriptional co-activator [9]. During oxidative stress, DJ-1 has been demonstrated to modulate the expression of genes such as glutamate cysteine ligase, extracellular superoxide dismutase (SOD3), or MnSOD [10–12]. DJ-1 also represses Bax expression through p53 interaction and exerts cytoprotection against Bax-induced, caspase-dependent cell death [13]. Our laboratory has previously shown that 6-OHDA triggers ROS-mediated apoptotic signaling in primary cultures of mesencephalic neurons, MN9D dopaminergic neurons, and rat brain models of PD [14–16]. In the present study, we aimed to identify an array of proteins that may be directly or indirectly regulated by DJ-1 under oxidative stress. To accomplish this, DJ-1 knockdown cells were established by stably introducing DJ-1 shRNA into MN9D cells and were subsequently subjected to 6-OHDA treatment. By applying two-dimensional electrophoresis (2-DE) in conjunction with matrix-assisted laser desorption/ionization time-of-flight (MALDI-TOF) analyses, we identified several proteins with altered expression in DJ-1 knockdown cells. Interestingly, our data suggest that increases in pro-apoptotic proteins and decreases in anti-apoptotic proteins may render DJ-1 knockdown cells more susceptible to oxidative stress.

Abbreviations: 6-OHDA, 6-hydroxydopamine; ROS, reactive oxygen species; PD, Parkinson's disease; SOD3, extracellular superoxide dismutase; 2-DE, 2-dimensional electrophoresis; MALDI-TOF, matrix-assisted laser desorption/ionization time-of-flight; PYGB, glycogen phosphorylase; SEPHS1, selenophosphate synthetase 1.

* Corresponding author at: Yonsei University College of Life Science and Biotechnology, Department of Systems Biology, 134 Shincheon-dong Seodaemoon-gu, Seoul 120-749, Republic of Korea. Fax: +8223125657.

E-mail address: yjoh@yonsei.ac.kr (Y.J. Oh).

0006-291X/$ - see front matter © 2012 Elsevier Inc. All rights reserved.
http://dx.doi.org/10.1016/j.bbrc.2012.04.063

2. Materials and methods

2.1. Cell culture, drug treatment, and MTT reduction assay

MN9D cells stably expressing DJ-1 shRNA were established. Stably transfected cells were plated on 25 μg/ml poly-D-lysine-coated culture dishes and cultivated in Dulbecco's modified Eagle's medium (DMEM; Sigma, St. Louis, MO) supplemented with 10% heat-inactivated fetal bovine serum (Gibco, Grand Island, NY) and 500 μg/ml G-418 (A.G. Scientific, San Diego, CA) in an atmosphere of 10% CO_2 for 2–3 days. The cells were then switched to serum-free N2 supplement with or without 100 μM 6-OHDA (Sigma). The rate of cell survival was determined by the 3-[4,5-dimethylthiazol-2-yl]-2,5-diphenyltetrazolium bromide (MTT) reduction assay as described previously [16].

2.2. DNA constructs and transfection

For gene silencing studies, MN9D cells were transfected with DJ-1 shRNA constructs within a pRNA-U6.1/Neo vector (GenScript Corporation, Piscataway, NJ), which contained a small DJ-1 hairpin RNA and green fluorescent protein as a reporter sequence. The target sequences used were 5′-GTGATTCCTGTGGATGTCATG-3′ (nucleotides 58–79). To establish the stable cell lines, MN9D cells were transfected with the above-mentioned vector using Lipofectamine 2000 (Invitrogen, Carlsbad, CA) and cultivated in medium containing 500 μg/ml G418. For control cells, the pRNA-U6.1/Neo vector harboring a firefly shRNA (5′-CTTACGCTGAGTACTTCGA-3′) were used, and all the G418-resistant population were pooled. For the luciferase reporter assay, the construct for the promoter region (−2 kbp) of glycogen phosphorylase (gene name: PYGB) was created from genomic DNA from MN9D cell lysates with the following a pair of primers: 5′-GAGGTACCTTACAGGAGGCAGCACTGTATATC-3′ and 5′-ATCAAGCTTGCAGAGAAGACTCTAGCGC-3′. KpnI and HindIII sites were added to the forward and reverse primers, respectively. The PCR product was introduced into a pGL4.17 [*luc2*/Neo] vector (Promega, Madison, WI).

2.3. ROS measurement

MN9D cells stably expressing DJ-1 shRNA or the firefly shRNA were incubated with or without 100 μM 6-OHDA for 6 h. The cells were then incubated with DMEM containing 50 μM dihydroethidium (Invitrogen) for 30 min at 37 °C and subsequently washed twice with DMEM. Fluorescent images were taken with an Axiovert 100 microscope (Carl Zeiss, Jena, Germany).

2.4. 2-DE and mass spectrometry

Unless otherwise stated, all chemicals for 2-DE were purchased from Sigma. As previously described [15], 2-DE was performed using MN9D control and DJ-1 knockdown cells treated with or without 100 μM 6-OHDA for 12 h. Briefly, the cells were solubilized in a sample buffer containing 5 M urea, 2 M thiourea, 2% CHAPS, 0.25% Tween 20, 100 mM dithiothreitol, 10% isopropyl alcohol, 12.5% water-saturated butanol, 5% glycerol, and a protease inhibitor cocktail (Roche, Basel, Switzerland). The protein content was determined by a 2-D Quant kit (GE Healthcare, Uppsala, Sweden). The samples were diluted to a total volume of 500 μl lysis buffer containing 1% IPG buffer for pH 4–7 linear Immobiline Drystrip (24 cm; GE healthcare) and rehydrated at room temperature overnight. The gels were run for a total of 100 kV-h using progressively increasing voltage on an Ettan IPGphor (GE healthcare). After equilibration, sodium dodecyl sulfate polyacrylamide gel electrophoresis (SDS–PAGE) was performed on an 8–18% gradient gel in an Ettan Dalt II System for 16 h at 18 mA/gel and stopped

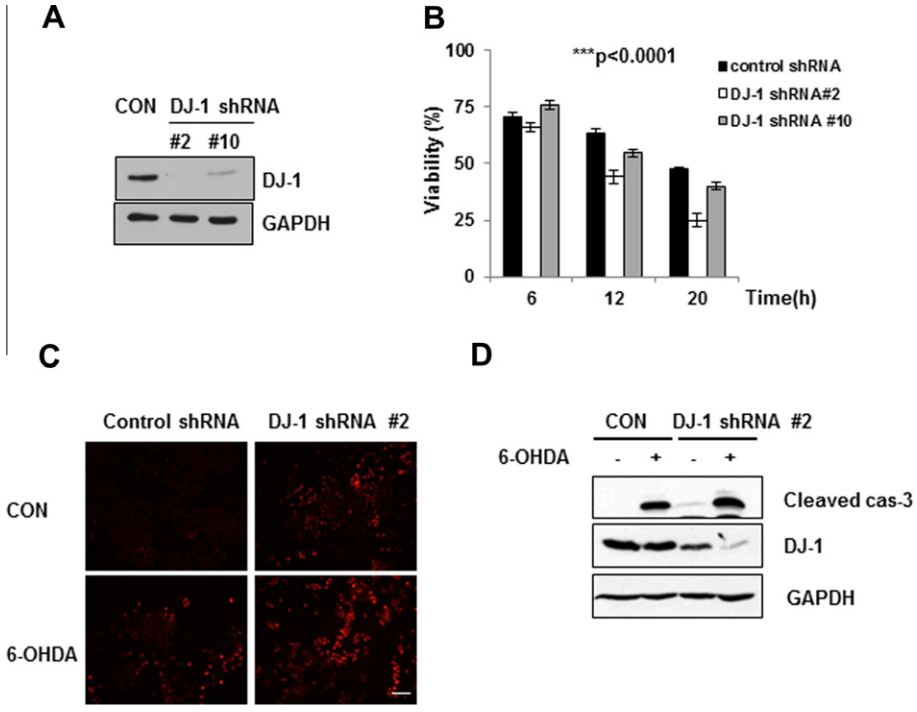

Fig. 1. Characterization of DJ-1 knockdown MN9D dopaminergic neurons. (A) Total cell lysates in MN9D cells stably expressing control sequences (CON) or DJ-1 shRNA constructs (clones #2 and #10) were immunoblotted using an anti-DJ-1 antibody. Anti-GAPDH antibody was used as a loading control. (B) Cells were treated with or without 100 μM 6-OHDA for the indicated time periods. Viability was measured by an MTT reduction assay. Values from each treatment are expressed as a percentage of the untreated cells (100%). Significant differences were determined by two-way ANOVA and Bonferroni post-tests. $^{***}p < 0.0001$. (C) Following 6-OHDA treatment for 6 h, cells were incubated with 50 μM dihydroethidium, an ROS-sensitive fluorescent dye. The scale bar represents 100 μm. (D) Cells were treated with 100 μM 6-OHDA for 12 h and subjected to immunoblot analyses using antibodies that recognize cleaved caspase-3, DJ-1, and GAPDH. Blots are representative of three independent experiments.

Table 1
Summary of the identified proteins altered in DJ-1 knockdown cells.

Spot No.	Protein name[a]	Accession number[b]	Protein mass/pI[c] *Da/pI*	Mowse score	Matched peptide	Sequence coverage *%*
1	Protein disulfide-isomerase precursor	P09103	57144/4.8	7.83E+14	24 (26)	45
3	40S ribosomal protein SA (p40)	P14206	32588/4.7	4.43E+08	13 (10)	46
4	Galectin-1	P16045	14735/5.3	1.12E+07	8 (3)	67
5	Adenylate kinase isoenzyme 1	Q9R0Y5	21540/5.7	6.09E+08	10 (9)	59
8	Proteasome activator complex subunit 1	P97371	28673/5.7	1.08E+10	16 (12)	60
9	NG,NG-dimethylarginine dimethylaminohydrolase 2	Q99LD8	29646/5.7	4.20E+07	11 (10)	49
10	Stathmin	P54227	17143/5.8	679062	12 (15)	55
14	Galectin-7	O54974	15173/6.7	1178	4(6)	41
15	D-3-phosphoglycerate dehydrogenase	Q61753	56455/6.1	1.24E+06	12 (15)	18
17	Prefoldin subunit 1	Q9CWM4	14255/7.9	1.97E+08	12 (20)	63
18	Alpha-enolase	P17182	47010/6.4	2.82E+13	17 (21)	49
20	Stress-induced-phosphoprotein 1	Q60864	62583/6.4	3.83E+13	29 (26)	42
33	Calumenin precursor	O35887	37064/4.5	7.13E+09	15 (18)	54
37	Peroxiredoxin-2	Q61171	21648/5.2	1.18E+05	7 (9)	31
38	Ubiquitin carboxyl-terminal hydrolase isozyme L1	Q9R0P9	24838/5.1	3.10E+07	13 (11)	53
39	Inorganic pyrophosphatase	Q9D819	32667/5.4	2.25E+12	21 (23)	59
40	Calponin-3	Q9DAW9	36429/5.5	5.46E+09	15 (13)	41
41	Selenophosphate synthetase 1	Q8BH69	42907/5.6	1.41E+11	15 (19)	47
42	Platelet-activating factor acetylhydrolase IB beta subunit	Q61206	25492/5.8	1.87E+06	12 (16)	58
43	Ubiquitin carboxyl-terminal hydrolase isozyme L1	Q9R0P9	24838/5.1	1.01E+08	12 (11)	41
44	Glycogen phosphorylase, brain form	Q8CI94	96600/6.3	1.07E+07	14 (10)	15
45	Stathmin	P54227	17143/5.8	1.10E+05	10 (12)	49
47	Transgelin-2	Q9WVA4	23466/6.8	1.32E+10	14 (20)	59
48	Prefoldin subunit 3	P61759	22436/6.0	7.91E+10	17 (22)	52
49	Peroxiredoxin-6	O08709	24740/5.7	5.39E+13	20(25)	71
51	Heterogeneous nuclear ribonucleoprotein K	P61979	50977/5.4	1.89E+10	20 (21)	33
52	ATP synthase coupling factor 6, mitochondrial precursor	P97450	12497/9.4	7.67E+04	6 (9)	43

[a] Each protein spot was identified based on mass spectra of tryptic peptides obtained by MALDI-TOF mass spectrometry.
[b] Accession numbers of the identified protein spots were obtained from the Swiss-Prot data base.
[c] Theoretical molecular mass (Da) and pI.

just before the dye front ran off the gels. The gels were then stained with 0.1% Coomassie Brilliant blue G-250 and analyzed using the Proteom Weaver software system version 2.1 (DEFINIENS, München, Germany). Protein spots of interest were manually excised from the gel and processed by enzymatic digestion with 10 μg/ml trypsin (Promega) in 25 mM NH_4HCO_3 for 18 h at 37 °C. The peptides were solubilized with 0.1% trifluoroacetic acid and desalted using an in-house column packed with C18 porous beads. Bound peptides were eluted in 0.6 μl elution buffer and spotted onto a MALDI plate (Applied Biosystems, Foster City, CA). For mass spectrometry, peptide mixtures were analyzed by a 4700 Proteomics Analyzer (Applied Biosystems). The peptide masses were matched with the theoretical peptide masses of all proteins from the mouse species using either the Swiss-Prot or UniProt databases.

2.5. Immunoblot analysis

The cells were lysed with RIPA buffer containing 0.1% SDS and complete protease inhibitor cocktail (Roche). The lysates were homogenized using a 1-ml syringe with a 26-gauge needle. The protein content was quantified using the Bradford protein assay reagent (Bio-Rad, Hercules, CA). Predetermined amounts of proteins were separated on 12.5% SDS–PAGE gels and blotted onto pre-wetted PVDF membranes. The membranes were incubated with one of the following antibodies at 4 °C overnight: goat anti-DJ-1 (1:2000; Abcam, Cambridge, MA), rabbit anti-cleaved caspase-3 (1:3000; Cell Signaling, Beverly, MA), rabbit anti-galectin-7 (1:1000; Bethyl Laboratories, Inc., Montgomery, TX), and rabbit anti-peroxiredoxin-6 (1:1000; LabFrontier, Seoul, Korea). A mouse anti-GAPDH antibody (Millipore, Billerica, MA; 1:3000) and a rabbit anti-actin antibody (Sigma; 1:3000) were used as loading controls. The horseradish peroxidase-conjugated secondary antibodies used included goat anti-rabbit and anti-mouse IgGs (1:5000; Santa Cruz Biotechnology, Santa Cruz, CA), or donkey anti-goat IgG (1:20,000; Abcam). Enhanced chemiluminescence (PerkinElmer Inc., Waltham, MA) was used for detecting specific bands. Relative band intensities were measured using Image J software (NIH, Bethesda, MD).

2.6. RNA isolation and RT-PCR

Total RNA was isolated using TRIzol® reagent (Invitrogen) according to the protocol provided by the manufacturer. A portion of the total RNA was reverse transcribed using M-MLV Reverse-transcriptase (Promega). PCR was performed using 10 pmol of a pair of each primer: calponin, 5′-ATGACCCACTTCAACAAGGGCC-3′ and 5′-CTAATAATCAATGCCCTGGTCGTCG-3′; glycogen phosphorylase (PYGB), 5′-TACAAGGTGAAGATCAACCC-3′ and 5′-GATCATCTTAGCCATGTGGT-3′; and selenophosphate synthetase 1 (SEPHS1) 5′-ATGTCTACTCGAGAGTCCTTTAACCCG-3′ and 5′-GGAGGTGGCAACCAGGTGTG-3′. Gene-specific fragments were obtained by linear phase PCR amplification and normalized for 18s rRNA levels measured with 18S Primer and Competimer (Ambion, Austin, TX). The PCR products were resolved on 1.5% agarose gels and visualized after staining with ethidium bromide.

2.7. Luciferase reporter assay

The cells were transfected with a total of 4 μg DNA using Lipofectamine 2000. The plasmids used for transfection included pGL4.17 [*luc2*/Neo] or pGL4.17 [*luc2*/PGYB]. Cells were co-transfected with pGL4.73 [*hRluc*/SV40], which constitutively expresses Renilla luciferase, to normalize transfection efficiency. Twenty-four hours after transfection, the cells were treated with 100 μM 6-OHDA for 12 h. After drug treatment, the cells were lysed and analyzed using the Dual-Luciferase Reporter Assay system (Promega).

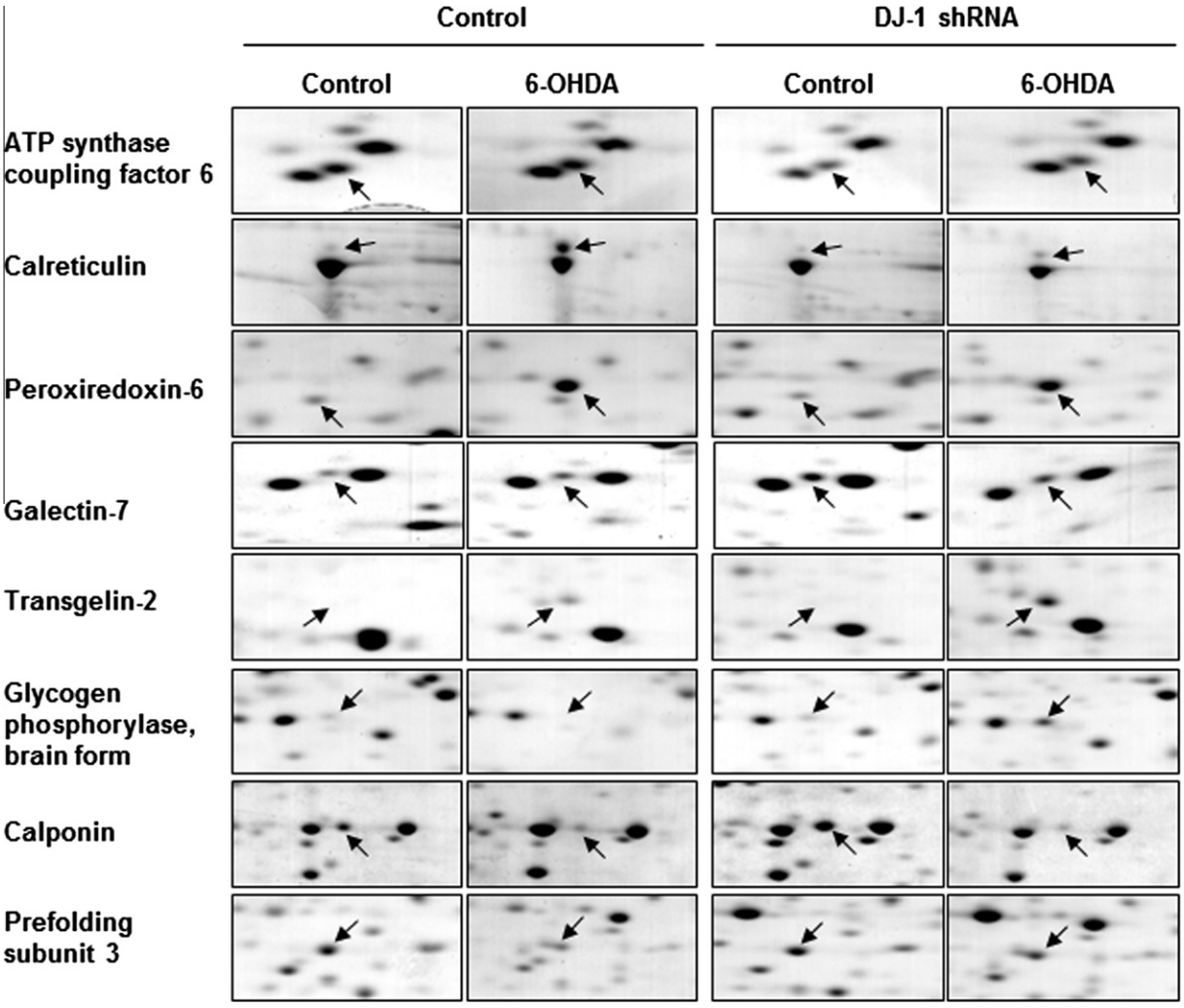

Fig. 2. Comparative close-up views of altered protein spots. MN9D cells stably expressing either the control vector or DJ-1 shRNA constructs (clone #2) were treated with or without 100 μM 6-OHDA for 12 h. Total cell lysates (1.5 mg) were separated by 2-DE and stained with 0.1% Coomassie Brilliant blue G-250. Among more than 1100 protein spots, enlarged views of eight representative protein spots altered in the DJ-1-deficient cells are shown. The arrows indicate the altered protein spots in each gel.

2.8. Statistics

The data are presented as mean ± standard deviation (SD). Significant differences were determined by Student's *t*-tests or two-way analysis of variance (ANOVA) and Bonferroni post-tests with GraphPad Prism 5 (GraphPad Software, San Diego, CA). Values of $^{***}p < 0.0001$, $^{**}p < 0.001$, and $^{*}p < 0.05$ were considered statistically significant.

3. Results

We established the stable knockdown cell lines by transfection with a vector expressing DJ-1 shRNA. As shown in Fig. 1A, the two clones, designated #2 and #10, showed significantly decreased expression levels of DJ-1 compared to the MN9D control cells. To further characterize the DJ-1 knockdown cells, we performed multiple assays to monitor cell viability, ROS generation, and activation of caspase-3. As shown in Fig. 1B, DJ-1 knockdown accelerated 6-OHDA-induced cell death (e.g., 63.3 ± 2.0%, 44.1 ± 3.0% or 57.5 ± 1.6% at 12 h; 48.9 ± 0.5%, 24.8 ± 2.9% or 43.5 ± 1.8% survival at 20 h for MN9D control cells, DJ-1 knockdown line #2, and #10, respectively). We next investigated whether the decreased DJ-1 levels correlated with increased ROS generation. Using an ROS-sensitive fluorescent dye, we found that the intensity of fluorescent signals increased even without 6-OHDA and increased even further after 6-OHDA treatment in DJ-1 knockdown cells (Fig. 1C). We previously demonstrated that 6-OHDA induces caspase-3-dependent apoptosis [14]. Therefore, we examined whether the decreased DJ-1 could further promote caspase-3 activation following 6-OHDA treatment. As anticipated, DJ-1 knockdown cells treated with 6-OHDA showed higher levels of cleaved caspase-3 compared to control cells (Fig. 1D). These results suggest that DJ-1 knockdown accelerates 6-OHDA-mediated cell death through the activation of ROS-mediated death signaling. These data are in line with the previous hypothesis that DJ-1 plays a protective role by decreasing ROS [17].

Using controls and the DJ-1-knockdown clone #2 treated with or without 6-OHDA for 12 h, we performed proteomic analysis using protein separation by 2-DE and identification by MALDI-TOF mass spectrometry. The typical Coomassie Blue-stained gels for each condition are shown in Supplementary Fig. 1. More than 1100 matched protein spots ranging from 10 to 100 kDa were detected in a 24-cm gel with a pI range of 4–7. Among these, the expression of 27 protein spots was significantly altered. These protein spots were then sequentially subjected to in-gel digestion with trypsin, MALDI-TOF mass spectrometry, and a search with either the NCBI or Swiss-Prot databases. Table 1 summarizes the

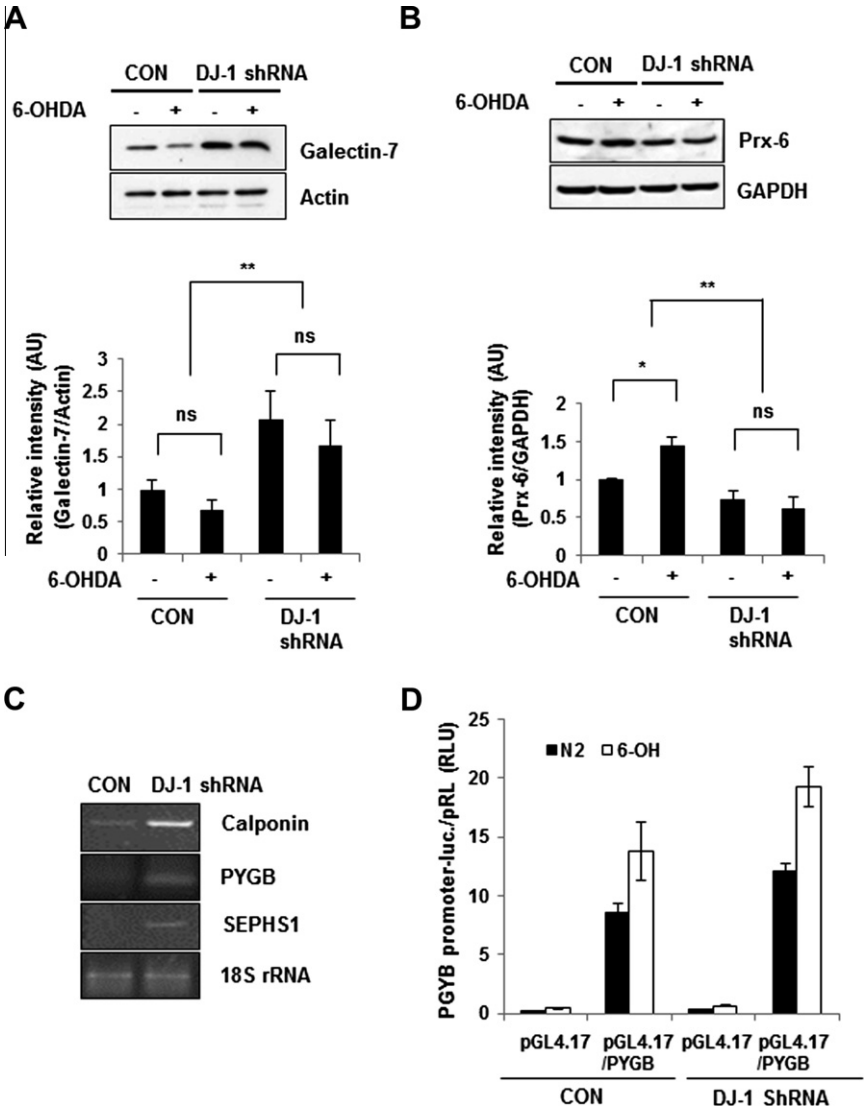

Fig. 3. Expression patterns of the identified proteins and transcriptional regulation of the DJ-1 target genes. (A and B) Cells were treated with 100 μM 6-OHDA for 12 h and subjected to immunoblot analyses for (A) galectin-7 and (B) peroxiredoxin-6 (Prx-6). Rabbit anti-actin and mouse anti-GAPDH antibodies were utilized as loading controls. Quantitative analysis of the relative intensity of galectin-7 and peroxiredoxin-6 was performed. Each bar represents the mean ± SD from three independent experiments. Significance was determined by two-way ANOVA. $^{**}p < 0.001$; $^{*}p < 0.05$; ns, not significant. (C) Semiquantitative RT-PCR was performed using total RNA harvested from control or DJ-1-deficient MN9D cells. RT-PCR products were resolved on 1.5% agarose gels and visualized after staining with ethidium bromide. 18s rRNA was used as an internal control. (D) A luciferase reporter assay was performed using the reporter plasmids containing the promoter region of PYGB. Relative luminescence units (RLU) of the PYGB reporter were normalized by Renilla luciferase activity. The graph represents the mean ± SD from two independent experiments.

information regarding these identified proteins, including the accession number, protein mass/pI, MOWSE score, matched peptide, and sequence coverage. Close-up views of the eight representative regions are presented in Fig. 2.

Due to their proposed roles in modulating apoptosis and ROS scavenging [18–21], we further confirmed the expression levels of galectin-7 and peroxiredoxin-6. As shown in Fig. 3A, immunoblot analyses indicated that basal levels of galectin-7 increased up to 2.06-fold in DJ-1 knockdown cells. Following drug treatment, a slight decrease in galectin-7 was detected in both cell types; however, larger levels of galectin-7 remained in the DJ-1 knockdown cells treated with 6-OHDA. Regardless of 6-OHDA treatment, DJ-1-knockdown cells showed decreased levels of peroxiredoxin-6 (Fig. 3B). Interestingly, 6-OHDA treatment caused a marked decrease of peroxiredoxin-6 in DJ-1 knockdown cells by more than 2.3-fold compared to 6-OHDA-treated control cells.

Emerging evidence supports the theory that p53 plays a critical role in neuronal cell death associated with PD [22–25]. Based on a study showing that neurons in DJ-1-null zebra fish have increased levels of p53 [26], we hypothesized that DJ-1 may mediate the pro-apoptotic activity of p53. To identify p53 target proteins potentially regulated by DJ-1, we analyzed the promoter region of the identified proteins using a p53MH algorism [27]. The genes glycogen phosphorylase (PYGB) and selenophosphate synthetase 1 (SEPHS1) contain p53 binding sites within their promoters (Supplementary Fig. 2). Furthermore, their scores were as high as those of well-known p53 targets p21 and siah1. To evaluate the mRNA levels of PYGB and SEPHS1, we performed semi-quantitative RT-PCR using RNA from control or DJ-1 knockdown MN9D cells. Similar to the results obtained from the 2DE analysis, the mRNA levels of PYGB and SEPHS1 increased in DJ-1 knockdown cells (Fig. 3C). To further investigate whether the observed increase in PYGB mRNA was caused by an increase in transcriptional activity, luciferase analysis was performed after 6-OHDA treatment for 12 h using cells transiently transfected with a luciferase-reporter vector containing the PYGB promoter. As shown in Fig. 3D, PYGB promoter

activity increased following 6-OHDA treatment in both cell types, and this increase was higher in DJ-1-knockdown cells, suggesting that DJ-1 plays a role in inhibiting the expression of p53 target genes that are associated with cell death.

4. Discussion

Here, we demonstrated that the loss of DJ-1 led to an increase in ROS generation and the acceleration of 6-OHDA-mediated apoptosis. Proteomic analyses revealed that the expression levels of 27 protein spots either increased or decreased in DJ-1-deficient cells. These altered proteins encompass a range of anti-oxidant proteins, pro-apoptotic proteins, components of the mitochondrial electron transport chain, and glucose metabolism-related proteins. As confirmed by immunoblot analyses, the expression level of galectin-7 increased while peroxiredoxin-6 decreased in DJ-1-deficient cells regardless of drug treatment. Upon 6-OHDA treatment, the expression level of galectin-7 increased up to 2-fold in DJ-1-deficient cells compared to control cells. In contrast, the level of peroxiredoxin-6 in 6-OHDA-treated DJ-1-deficient cells was less than 44% of the amount detected in 6-OHDA-treated control cells. Interestingly, it has been demonstrated that the overexpression of galectin-7 renders cells more sensitive to apoptosis under various stressful conditions. For example, galectin-7 plays a pro-apoptotic role by activating JNK and cytochrome c release to subsequently increase caspase-3-dependent apoptosis [18]. Peroxiredoxins have been shown to use the cysteine active site to convert harmful peroxides into harmless water [28]. Consequently, peroxiredoxins play an important role in reducing ROS in physiological and pathological conditions. More specifically, elevated expression of peroxiredoxin-6 exerts protective antioxidant defense and inhibits apoptosis [19–21]. Taken together, our data suggest that the susceptibility of DJ-1-deficient cells to apoptosis in response to 6-OHDA may be due to the altered expression of galectin-7 and peroxiredoxin-6. Therefore, DJ-1 may exert its protective effects by regulating the expression ratios of pro-apoptotic and anti-apoptotic proteins during oxidative stress-mediated cell death.

The tumor suppressor protein p53 plays an important role in cell-cycle arrest, apoptosis, and senescence in response to genotoxic and oxidative stress [29]. Specifically, p53 can directly regulate the expression of various genes to mediate p53-dependent cell cycle arrest and apoptosis. It is well established that p53 plays a key role in cellular responses to oxidative stress. Upon basal or low level oxidative stress, p53 regulates the expression of genes involved in regulating oxidative stress, including Sestrin, glutathione peroxidase, and aldehyde dehydrogenase. In response to high doses of oxidative stressors, p53 increases ROS levels and promotes apoptosis by inducing the expression of pro-oxidative genes, such as p53-induced gene 3, Bax, and Puma, and the suppression of antioxidant genes, such as superoxide dismutase 2 and NAD(P)H dehydrogenase [30]. Here, we found that both SEPHS1 and PYGB possess p53 binding sites, and their transcription levels increased in DJ-1-deficient cells. Previous studies have demonstrated that SEPHS is associated with hypersensitivity to ROS in the fly [31] and sensitizes cancer cells to ionizing radiation leading to apoptosis [32]. PYGB is predominantly distributed in the liver, skeletal muscle and brain. At the cellular level, the brain forms of PYGB exist primarily in astrocytes and certain neuronal populations [33]. Although direct evidence for a regulatory role in ROS generation and apoptosis has not been thoroughly investigated, PYGB has been implicated in oxidative stress and aging processes in yeast [34]. Importantly, the identification of p53 target genes among the 27 identified candidates in the present study raises the possibility that DJ-1 exerts a cytoprotective role by modulating p53-mediated cell death pathways.

Considering other decreased proteins associated with mitochondrial function (e.g., ATP synthase coupling factor 6) in DJ-1-deficient cells, our results suggest that DJ-1-deficiency may be closely linked to oxidative stress-induced apoptotic signaling and mitochondrial dysfunction. Further examination of mitochondrial and/or extramitochondrial pathways in this context will expand our understanding of the mechanisms mediating the protective role of DJ-1 during dopaminergic neurodegeneration.

Acknowledgments

This work was supported by a grant from the Ministry for Health, Welfare, and Family Affairs (A090063).

Appendix A. Supplementary data

Supplementary data associated with this article can be found, in the online version, at http://dx.doi.org/10.1016/j.bbrc.2012.04.063.

References

[1] W. Dauer, S. Przedborski, Parkinson's disease: mechanisms and models, Neuron 39 (2003) 889–909.
[2] J. Hardy, P. Lewis, T. Revesz, A. Lees, C. Paisan-Ruiz, The genetics of Parkinson's syndromes: a critical review, Curr. Opin. Genet. Dev. 19 (2009) 254–265.
[3] C.M. van Duijn, M.C. Dekker, V. Bonifati, R.J. Galjaard, J.J. Houwing-Duistermaat, P.J. Snijders, L. Testers, G.J. Breedveld, M. Horstink, L.A. Sandkuijl, J.C. van Swieten, B.A. Oostra, P. Heutink, Park7, a novel locus for autosomal recessive early-onset parkinsonism, on chromosome 1p36, Am. J. Hum. Genet. 69 (2001) 629–634.
[4] V. Bonifati, P. Rizzu, M.J. van Baren, O. Schaap, G.J. Breedveld, E. Krieger, M.C. Dekker, F. Squitieri, P. Ibanez, M. Joosse, J.W. van Dongen, N. Vanacore, J.C. van Swieten, A. Brice, G. Meco, C.M. van Duijn, B.A. Oostra, P. Heutink, Mutations in the DJ-1 gene associated with autosomal recessive early-onset parkinsonism, Science 299 (2003) 256–259.
[5] P.J. Kahle, J. Waak, T. Gasser, DJ-1 and prevention of oxidative stress in Parkinson's disease and other age-related disorders, Free Radic. Biol. Med. 47 (2009) 1354–1361.
[6] R.M. Canet-Aviles, M.A. Wilson, D.W. Miller, R. Ahmad, C. McLendon, S. Bandyopadhyay, M.J. Baptista, D. Ringe, G.A. Petsko, M.R. Cookson, The Parkinson's disease protein DJ-1 is neuroprotective due to cysteine–sulfinic acid-driven mitochondrial localization, Proc. Natl. Acad. Sci. USA 101 (2004) 9103–9108.
[7] K.J. Thomas, M.K. McCoy, J. Blackinton, A. Beilina, M. van der Brug, A. Sandebring, D. Miller, D. Maric, A. Cedazo-Minguez, M.R. Cookson, DJ-1 acts in parallel to the PINK1/parkin pathway to control mitochondrial function and autophagy, Hum. Mol. Genet. 20 (2011) 40–50.
[8] G. Krebiehl, S. Ruckerbauer, L.F. Burbulla, N. Kieper, B. Maurer, J. Waak, H. Wolburg, Z. Gizatullina, F.N. Gellerich, D. Woitalla, O. Riess, P.J. Kahle, T. Proikas-Cezanne, R. Kruger, Reduced basal autophagy and impaired mitochondrial dynamics due to loss of Parkinson's disease-associated protein DJ-1, Plos One 5 (2010).
[9] J. Xu, N. Zhong, H. Wang, J.E. Elias, C.Y. Kim, I. Woldman, C. Pifl, S.P. Gygi, C. Geula, B.A. Yankner, The Parkinson's disease-associated DJ-1 protein is a transcriptional co-activator that protects against neuronal apoptosis, Hum. Mol. Genet. 14 (2005) 1231–1241.
[10] H. Nishinaga, K. Takahashi-Niki, T. Taira, A. Andreadis, S.M. Iguchi-Ariga, H. Ariga, Expression profiles of genes in DJ-1-knockdown and L 166 P DJ-1 mutant cells, Neurosci. Lett. 390 (2005) 54–59.
[11] W. Zhou, C.R. Freed, DJ-1 up-regulates glutathione synthesis during oxidative stress and inhibits A53T alpha-synuclein toxicity, J. Biol. Chem. 280 (2005) 43150–43158.
[12] N. Zhong, J. Xu, Synergistic activation of the human MnSOD promoter by DJ-1 and PGC-1alpha: regulation by SUMOylation and oxidation, Hum. Mol. Genet. 17 (2008) 3357–3367.
[13] J. Fan, H. Ren, N. Jia, E. Fei, T. Zhou, P. Jiang, M. Wu, G. Wang, DJ-1 decreases Bax expression through repressing p53 transcriptional activity, J. Biol. Chem. 283 (2008) 4022–4030.
[14] B.S. Han, H.S. Hong, W.S. Choi, G.J. Markelonis, T.H. Oh, Y.J. Oh, Caspase-dependent and -independent cell death pathways in primary cultures of mesencephalic dopaminergic neurons after neurotoxin treatment, J. Neurosci. 23 (2003) 5069–5078.
[15] Y.M. Lee, S.H. Park, D.I. Shin, J.Y. Hwang, B. Park, Y.J. Park, T.H. Lee, H.Z. Chae, B.K. Jin, T.H. Oh, Y.J. Oh, Oxidative modification of peroxiredoxin is associated with drug-induced apoptotic signaling in experimental models of Parkinson disease, J. Biol. Chem. 283 (2008) 9986–9998.
[16] W.S. Choi, S.Y. Yoon, T.H. Oh, E.J. Choi, K.L. O'Malley, Y.J. Oh, Two distinct mechanisms are involved in 6-hydroxydopamine- and MPP+-induced

dopaminergic neuronal cell death: Role of caspases, ROS, and JNK, J. Neurosci. Res. 57 (1999) 86–94.
[17] T. Taira, Y. Saito, T. Niki, S.M.M. Iguchi-Ariga, K. Takahashi, H. Ariga, DJ-1 has a role in antioxidative stress to prevent cell death, EMBO Rep. 5 (2004) 213–218.
[18] I. Kuwabara, Y. Kuwabara, R.Y. Yang, M. Schuler, D.R. Green, B.L. Zuraw, D.K. Hsu, F.T. Liu, Galectin-7 (PIG1) exhibits pro-apoptotic function through JNK activation and mitochondrial cytochrome c release, J. Biol. Chem. 277 (2002) 3487–3497.
[19] H. Choi, J.W. Chang, Y.K. Jung, Peroxiredoxin 6 interferes with TRAIL-induced death-inducing signaling complex formation by binding to death effector domain caspase, Cell Death Differ. 18 (2011) 405–414.
[20] S.Y. Kim, E. Chun, K.Y. Lee, Phospholipase A(2) of peroxiredoxin 6 has a critical role in tumor necrosis factor-induced apoptosis, Cell Death Differ. 18 (2011) 1573–1583.
[21] L. Da Silva-Azevedo, S. Jahne, C. Hoffmann, D. Stalder, M. Heller, A.R. Pries, A. Zakrzewicz, O. Baum, Up-regulation of the peroxiredoxin-6 related metabolism of reactive oxygen species in skeletal muscle of mice lacking neuronal nitric oxide synthase, J. Physiol. London 587 (2009) 655–668.
[22] D. Blum, Y. Wu, M.F. Nissou, S. Arnaud, A.L. Benabid, J.M. Verna, P53 and Bax activation in 6-hydroxydopamine-induced apoptosis in PC12 cells, Brain Res. 751 (1997) 139–142.
[23] A.S. Mandir, C.M. Simbulan-Rosenthal, M.F. Poitras, J.R. Lumpkin, V.L. Dawson, M.E. Smulson, T.M. Dawson, A novel in vivo post-translational modification of p53 by PARP-1 in MPTP-induced parkinsonism, J. Neurochem. 83 (2002) 186–192.
[24] W. Duan, X. Zhu, B. Ladenheim, Q.S. Yu, Z. Guo, J. Oyler, R.G. Cutler, J.L. Cadet, N.H. Greig, M.P. Mattson, P53 inhibitors preserve dopamine neurons and motor function in experimental parkinsonism, Ann. Neurol. 52 (2002) 597–606.
[25] V.D. Nair, Activation of p53 signaling initiates apoptotic death in a cellular model of Parkinson's disease, Apoptosis 11 (2006) 955–966.
[26] S. Bretaud, C. Allen, P.W. Ingham, O. Bandmann, P53-dependent neuronal cell death in a DJ-1-deficient zebrafish model of Parkinson's disease, J. Neurochem. 100 (2007) 1626–1635.
[27] J. Hoh, S. Jin, T. Parrado, J. Edington, A.J. Levine, J. Ott, The p53MH algorithm and its application in detecting p53-responsive genes, Proc. Natl. Acad. Sci. USA 99 (2002) 8467–8472.
[28] S.G. Rhee, H.Z. Chae, K. Kim, Peroxiredoxins: a historical overview and speculative preview of novel mechanisms and emerging concepts in cell signaling, Free Radic. Biol. Med. 38 (2005) 1543–1552.
[29] A.J. Levine, M. Oren, The first 30 years of p53: growing ever more complex, Nat. Rev. Cancer 9 (2009) 749–758.
[30] D. Liu, Y. Xu, P53, oxidative stress, and aging, Antioxid. Redo. Signal. 15 (2011) 1669–1678.
[31] M. Morey, M. Corominas, F. Serras, DIAP1 suppresses ROS-induced apoptosis caused by impairment of the selD/sps1 homolog in *Drosophila*, J. Cell Sci. 116 (2003) 4597–4604.
[32] H.J. Chung, S.I. Yoon, S.H. Shin, Y.A. Koh, S.J. Lee, Y.S. Lee, S. Bae, P53-Mediated enhancement of radiosensitivity by selenophosphate synthetase 1 overexpression, J. Cell Physiol. 209 (2006) 131–141.
[33] B. Pfeiffer-Guglielmi, B. Fleckenstein, G. Jung, B. Hamprecht, Immunocytochemical localization of glycogen phosphorylase isozymes in rat nervous tissues by using isozyme-specific antibodies, J. Neurochem. 85 (2003) 73–81.
[34] C. Favre, P.S. Aguilar, M.C. Carrillo, Oxidative stress and chronological aging in glycogen-phosphorylase-deleted yeast, Free Radic. Biol. Med. 45 (2008) 1446–1456.